2022

Measurement of dispersion and index of refraction of 1-decanol with spectrally resolved white light interferometry

Nathan G. Drouillard
University of Windsor

TJ Hammond
University of Windsor

Research Article | Vol. 30, No. 22 / 24 Oct 2022 / Optics Express 39407
Optics EXPRESS

Measurement of dispersion and index of refraction of 1-decanol with spectrally resolved white light interferometry

NATHAN G. DROUILLARD AND T. J. HAMMOND*

Dept. of Physics, University of Windsor, Windsor ON N9B 3P4, Canada
thammond@uwindsor.ca

Abstract: The high density, high nonlinearity, and stability of liquids make them an attractive medium for spectral broadening and supercontinuum generation in ultrafast experiments. To understand ultrashort pulse propagation in these media, their indices of refraction and dispersions must be characterized. We employ a Mach-Zehnder interferometer to generate a series of interferograms, which we refer to as a spectrogram, to develop a new method of using spectrally resolved white light interferometry to determine the refractive indices of materials. We determine the indices of refraction of BK7, sapphire, ethanol, and 1-decanol at 24°C across the visible and near infrared. To our knowledge, this is the first reported dispersion and index of refraction measurement of 1-decanol.

1. Introduction

Ultrashort laser pulses are bursts of radiation that last hundreds of femtoseconds (1 fs = 10^{-15} s) or shorter. Such ultrashort pulses require significant bandwidth, with spectra often spanning tens to hundreds of nanometers in the visible or near infrared [1–3]. However, controlling the phase across this spectrum becomes challenging due to the frequency dependent index of refraction of materials, known as dispersion. As the ultrashort pulse propagates through these dispersive materials, an initially compressed pulse increases in duration and decreases in peak intensity, limiting the time resolution of pump-probe experiments [4–6], and the nonlinearity for strong-field physics experiments [7–12]. Dispersion controls the temporal character of these ultrashort pulses, requiring its measurement in optical materials across the spectrum of interest.

Spectrally resolved white light interferometry (SRWLI) is a well-established method for measuring the index of refraction of materials [13–15]. From a single interferogram, it is possible to fit the phase across the spectrum, thus retrieving the index of refraction [16]. An interesting approach fits the phase of the oscillating interferogram, but the index must be independently measured at a given wavelength via some other calibrated technique [17,18]. Because the dispersion determines the fringe spacing in the interferograms, we also found that this method was difficult to use for thick and highly dispersive samples. Conversely, we can select a region with decreased fringe spacing by delaying the interferometer to match the group delay at a desired frequency allowing us to analyze thicker, more dispersive samples [15]. By mapping out the index for various desired frequencies, it is possible to stitch together the index of refraction (and simultaneously measure the group index over the spectrum) [17]. Another method of SRWLI generates a series interferograms while varying the sample thickness; the resulting spectrogram leads to a direct measurement of the index of refraction [19,20]. Because we are interested in the effect the material has on an ultrashort laser pulse, characterizing the dispersion is more important than the index itself. By scanning the delay of a reference arm, we can measure the dispersion directly [21,22]. In this paper, we modify this approach by combining it with SRWLI to measure the dispersion of 1-decanol, and use the results to reconstruct the index of refraction.

#473178 https://doi.org/10.1364/OE.473178
Journal © 2022 Received 16 Aug 2022; revised 19 Sep 2022; accepted 19 Sep 2022; published 10 Oct 2022

Optics EXPRESS

We previously reported that intense pulses from a Ti:Sapphire laser spectrally broaden in 1-decanol, demonstrating a simple approach to compress near infrared laser pulses from 100 fs to 30 fs [23]. Although 1-decanol is useful in pharmaceuticals showing improved drug delivery and low irritation [24] and as a solvent [25], its optical properties have not been studied. The high boiling point, high nonlinearity, and low toxicity of 1-decanol make it a novel material of interest for nonlinear optics when physical interaction with the material is likely. We test our measurement by comparing our results to literature for BK7, sapphire n_o (ordinary axis), and ethanol, and discuss our results of 1-decanol.

2. Theory

Light of frequency ω passing through an optic of thickness L with index of refraction $n(\omega)$ accumulates a phase $\phi(\omega) = \frac{\omega}{c}Ln(\omega)$, where c is the speed of light. To resolve this phase, we can compare it to a reference using an interferometer, where the phase difference of the two sources leads to an interference across the spectrum, and interferogram. The phase of the interferogram is [26,27],

$$\phi_i(\omega) = \frac{\omega}{c}L\Big(n(\omega) - n_g\Big) + 2\pi m, \tag{1}$$

where $n_g = n + \omega\partial n/\partial\omega$ is the group index of refraction evaluated at some reference frequency ω_0, and m is an integer. The unknown value of m leads to an ambiguity that prevents us from directly calculating the index from the phase. To simplify the measurement, our reference frequency is the point where the fringe spacing is maximized, referred to as stationary phase [15], where $\lambda_s = 2\pi c/\omega_0$ is the stationary phase wavelength. The resulting spectrogram is,

$$S(\omega, d) = I(\omega)\Big(1 + V(\omega)cos(\phi_i + \frac{\omega}{c}d)\Big), \tag{2}$$

where $I(\omega)$ is the source spectrum, $V(\omega)$ is the fringe visibility, and d is the interferometer stage position that compensates for the material group delay, $L_g = L(n_g - 1)$.

For each frequency component of the spectrogram, we subtract its mean value and normalize to create a sinusoidal function of d. We take the Hilbert transform and calculate the phase at $d = 0$. By this method, we measure the phase of each spectral component independently. We then unwrap the phase to create a continuous function, and fit it to a fifth order polynomial,

$$\begin{aligned}\phi_r(\omega) = \phi_0 + (\omega - \omega_0)D + \tfrac{(\omega-\omega_0)^2}{2}GDD + \tfrac{(\omega-\omega_0)^3}{6}TOD + \\ \tfrac{(\omega-\omega_0)^4}{24}FOD + \tfrac{(\omega-\omega_0)^5}{120}FID,\end{aligned} \tag{3}$$

where ϕ_0 is a constant phase offset, D is the group delay, GDD is the group delay dispersion, TOD is the third order dispersion, FOD is the fourth order dispersion, and FID is the fifth order dispersion. We can then directly calculate the material group velocity dispersion by dividing by L. We reconstruct the index, $n(\omega)$, by equating the two phases, $\phi_i(\omega) = \phi_r(\omega)$. The only unknown variable in Eq. (1) is $n(\omega)$, which we then fit to a modified Cauchy equation,

$$n(\lambda) = A + \frac{B}{\lambda^2} + C\lambda^2 + \frac{D}{\lambda^4} + E\lambda^4 + \frac{F}{\lambda^6}, \tag{4}$$

where $\lambda = 2\pi c/\omega$ is the wavelength. We summarize this procedure in Fig. 1.

Optics EXPRESS

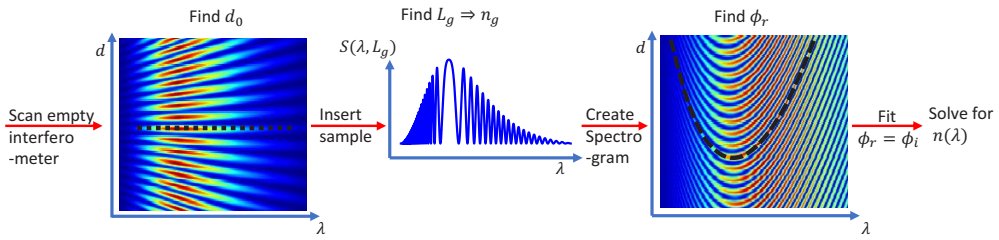

Fig. 1. Block diagram of the procedure to find $n(\lambda)$. We scan the empty interferometer to find d_0, the zero delay position (marked by the dotted line). We insert the sample in one arm and scan the delay to find the group delay, L_g, which leads to the group index, n_g. Around this point, we make a series of interferograms to create the spectrogram. From the spectrogram, we find the phase and fit it across the spectrum. Equating this retrieved phase, ϕ_r to the interferogram phase, ϕ_i leads to the index.

3. Measurement

The setup of our Mach-Zehnder interferometer is shown in Fig. 2. For the white light source (incandescent bulb), we use a halogen lamp that spans from 400 to beyond 1030 nm (the limit of our spectrometer). To improve the beam quality of the tungsten filament, we focus (f_1 = 250 mm) the light through a 300 µm pinhole and collimate the beam (f_2 = 250 mm); we found that the chromatic dispersion of lenses limited the bandwidth of the experiment and so opted for broadband silver focussing mirrors. To ensure a near-uniform reflection across the spectrum, a 5 mm thick CaF_2 window separates the two beams (BS). These thick windows ensure that we can discriminate between the front and back reflections to improve the fringe visibility, while the low dispersion of CaF_2 allows for near-uniform Fresnel reflection across the spectrum from the front surface. We compensate for any residual dispersion caused by the beam splitters/combiners with a dispersion compensating plate (DSP) in the reference arm; for solid samples this is a thin fused silica plate while for liquids it is an empty cuvette. The corner cube (CC_1) on the computer-controlled stage (Thorlabs PT1-Z8) with nanometer resolution scans the delay of the reference arm to create the spectrogram. We place the sample in the other arm, and the two beams are recombined at the beam combiner (BC), also a 5 mm thick CaF_2 window. We focus the beam using a lens (l) into a visible and near infrared spectrometer (Ocean Insight Flame-S) to measure the interference spectrum; measuring the spectra as a function of delay creates the spectrogram.

Despite the delay stage having nanometer resolution, we found that there was a consistent difference between the stage measured position and the actual position. To measure the actual position, we calibrated the stage using a helium neon (HeNe) laser with a central wavelength at λ_{HeNe} = 632.816 nm. By measuring the interference as a function of delay with 50 nm steps, we generate a spectrogram (interference spectra as a function of delay). From the HeNe spectrogram, we take the Hilbert transform to retrieve the reference phase, ϕ_r. We found retrieving the phase was more accurate this way than the $\cos^{-1}$ function because of the small changes in the intensity envelope over the duration of the experiment. We then calculate the actual stage delay as $d_r = \phi_r \lambda_{HeNe}/2\pi$. The resulting measurement is shown in Fig. 3. We calculate that over the delay (twice the stage movement) of 26 mm, there is a difference of approximately 200 µm, or nearly 1%. However, this discrepancy is not a constant value as a function of position, but the discrepancy is a constant (to within tens of nm) at a given stage position. We also note that there are regions of approximately 1.5 mm where the difference is only ±1 µm, followed by short regions of greater error. With this calibration, we can accurately measure the group delay to within hundreds of nanometers, ensuring that the stage delay is not a significant source of error.

Optics EXPRESS

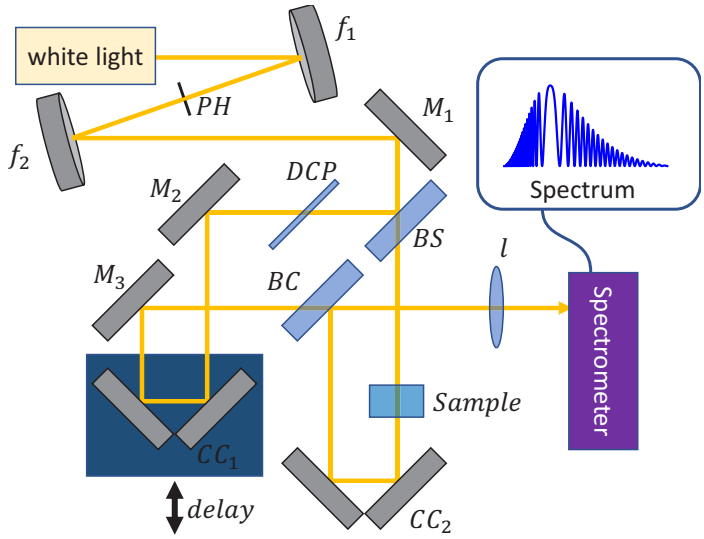

Fig. 2. Setup of the Mach-Zehnder interferometer. White light source is an incandescent bulb. Focusing silver mirrors, f_i, improve the beam quality and fringe visibility by passing through a pinhole, PH, and collimate the beam. M_i are flat silver mirrors, BS is beam splitter; BC is beam combiner; DCP is dispersion compensating plate; CC_i are corner cubes. Motorized delay stage creates reproducible spectrograms.

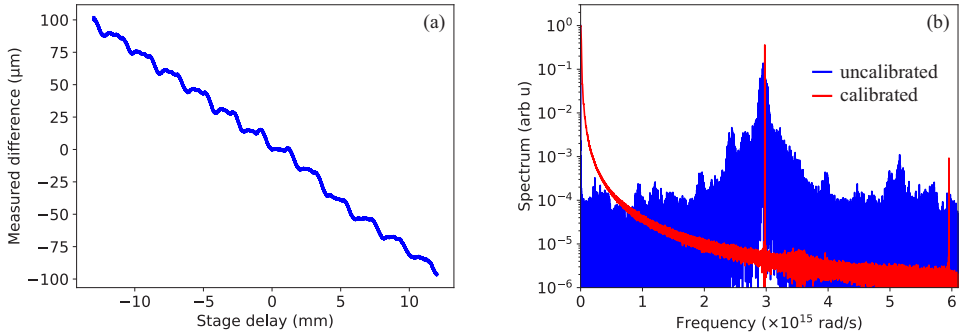

Fig. 3. Stage calibration with HeNe reference laser. (a) Measured difference in stage position from stage to reference. (b) Fourier transform of the spectrogram without (blue) and with (red) calibration.

In our Mach-Zehnder interferometer, 5 mm CaF_2 windows at 45° separate and combine the two beams. However, due to their thickness, we must measure and compensate for any residual dispersion. To this end, we measure the phase of the spectrogram of the dispersion compensated interferometer when the two arms are the same length (referred to as zero delay position, d_0), as shown in Fig. 4. The spectrogram shows a nearly perfectly straight interference pattern across the spectrum, implying that the dispersion is near zero. From the measured spectrogram phase, ϕ_i, we find that the balanced interferometer dispersion is $GDD = -1 \pm 2$ fs^2 across the observable spectrum.

Now that we have characterized the interferometer, we measure the dispersion and index of refraction of our samples. We place the sample under investigation in the fixed arm of the interferometer, and use the calibrated computer-controlled delay stage to find L_g. The stage is

Optics EXPRESS

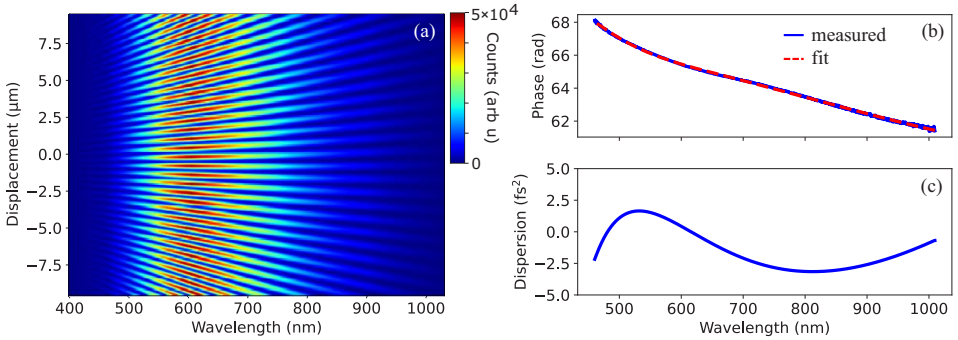

Fig. 4. Dispersion compensated Mach-Zehnder measurement. (a) Spectrogram of dispersion-compensated interferometer. (b) Retrieved phase (blue) and fit (red dashed). (c) Measured dispersion is near zero across the spectrum.

moved in the same direction for finding d_0 and for finding the group delay to minimize the effects of backlash. The group index is then measured to be

$$n_g(\omega_0) = \frac{L_g}{L} + 1 \tag{5}$$

The sample sizes with their uncertainty are listed in Table 1.

Table 1. Measured sample thickness

Sample	L (μm)	ΔL (μm)
BK7	5005	5
Sapphire n_o	5085	5
Ethanol	100280	10
1-Decanol	100280	10

Because we use thick samples, the relative thickness uncertainty is 0.1%. For the BK7 and sapphire samples, the uncertainty is 5 μm, as determined by the calipers. For the cuvette, we measure the thickness by measuring the cross-correlation signal of a 100 fs Ti:Sapphire laser. We take the difference in the back reflection of the front of the cuvette, and the front reflection of the back of the cuvette, to have an uncertainty of 10 μm. With the calibrated stage, the uncertainty in ΔL_g is estimated to be 200 nm, or $\Delta L_g/L_g$ is one to two orders of magnitude lower than $\Delta L/L$. We assume that the group index of air is unity.

As with the dispersion compensated case previously discussed, we scan the delay while measuring the interferogram to create a spectrogram. A sample spectrogram for BK7 is shown in Fig. 5. Again, we fit the phase for each frequency of the white light source, and use an unwrapping algorithm to make it continuous. We fit this phase, ϕ_r, to a fifth order polynomial; this fit allows us to accurately calculate the dispersion. Because the resolution of the spectrometer and the different dispersion of the various materials, we choose the stationary phase wavelength, λ_s, for the sample that yields sufficient fringe resolution over the broadest spectrum.

We list the measured group indices in Table 2, along with the measured dispersion values. We see good agreement between the measured n_g and the values reported in literature at the stationary phase wavelengths. We also report the measured four lowest orders of dispersion. Because the only approximation for the dispersion measurement is the polynomial fit, we obtain good agreement with literature. Although we measure the group delay dispersion, $\partial^2\phi/\partial\omega^2$, we

Optics EXPRESS

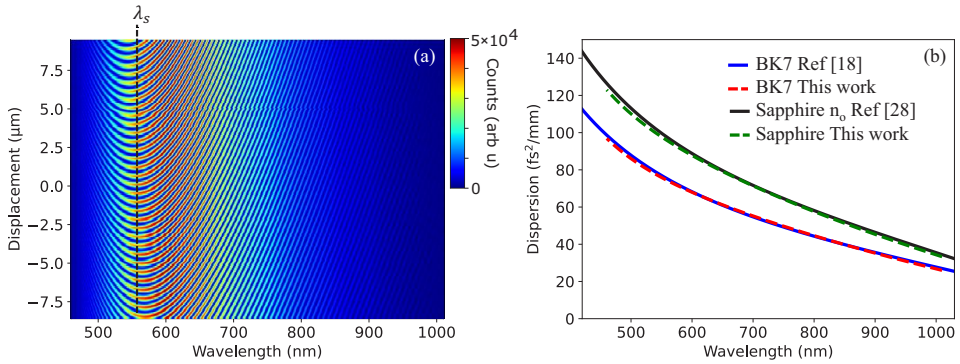

Fig. 5. Dispersion measurement of solid samples. (a) Spectrogram for BK7; the curvature of the interference pattern is indicative of a dispersive material. The minimum of the curvature, the stationary phase wavelength λ_s, has the greatest fringe visibility. (b) The retrieved dispersion for BK7 (red dashed) compared to literature (blue solid), and n_o sapphire (green dashed) compared to literature (black solid).

plot the group velocity dispersion, $\partial^2 k/\partial\omega^2$ where $\phi = kL$. With the largest uncertainty in the measurement stemming from ΔL, the estimated error is less than the linewidths in Fig. 5(b).

Table 2. The measured group delay, n_g, at the stationary phase wavelength, λ_s (nm), compared to the reference values[a]

Sample	λ_s	n_g	n_g Ref	GVD	TOD	FOD	FID
BK7	557	1.5440	1.5450 [18]	74.7	28.1	4.22	18.7
Sapphire n_o	588	1.8005	1.8006 [28]	90.0	35.0	1.51	21.3
Ethanol	602	1.3801	1.3788 [18]	53.8	21.3	1.2	1.75
1-Decanol	640	1.4514	NR	64.6	26.2	1.67	0

[a]The estimated error in n_g is 0.0005. We list the measured GVD (fs^2/mm) , TOD (fs^3/mm), FOD (fs^4/mm), and FID (fs^5/mm) from the phase fit; NR is not reported.

We present the results of our dispersion measurement for ethanol and 1-decanol in Fig. 6. We found that when comparing our results to literature, there is some discrepancy among the references. Because the density depends on the temperature, we speculate that the dispersion is sensitive to ambient conditions and requires further investigation that is beyond the scope of this work. The measured bandwidth of 1-decanol is narrower than ethanol because our spectrometer could not resolve the highly oscillating fringes in the interferogram in these regions because of the thick sample and higher dispersion. The dispersion of 1-decanol has a similar shape to ethanol, but is approximately 15 fs^2/mm higher throughout the measured spectra.

The reconstructed indices of refraction of BK7 and sapphire n_o are shown in Fig. 7. The BK7 curves correspond to the left axis (blue is Ref. [18], red is this work), where the thickness of the red line is the uncertainty in the index. Likewise, the sapphire n_o curves correspond to the right axis (black line is Ref. [28], green line is this work). We find good agreement between literature and our work; the index of BK7 slightly higher and outside the error at longer wavelengths, but the sapphire n_o is within the measurement error across the spectrum.

We also reconstruct the indices of refraction for ethanol and 1-decanol, as shown in Fig. 8. The ethanol curve corresponds to the left axis (blue is Ref. [18], red is this work). We find that our reconstructed indices agree well with Ref. [29] at 25°C, although at longer wavelengths the

Optics EXPRESS

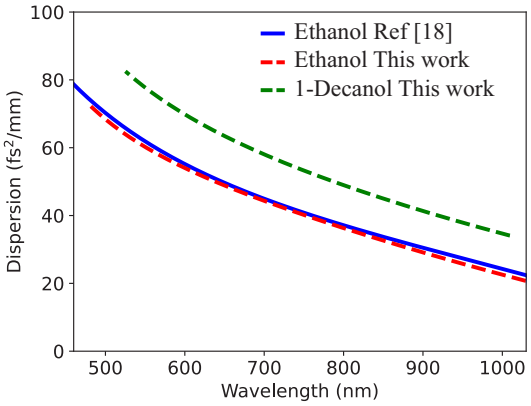

Fig. 6. Dispersion of ethanol and 1-decanol, comparing literature for ethanol (solid blue) to this work (red dashed). We report the dispersion for 1-decanol (green dashed).

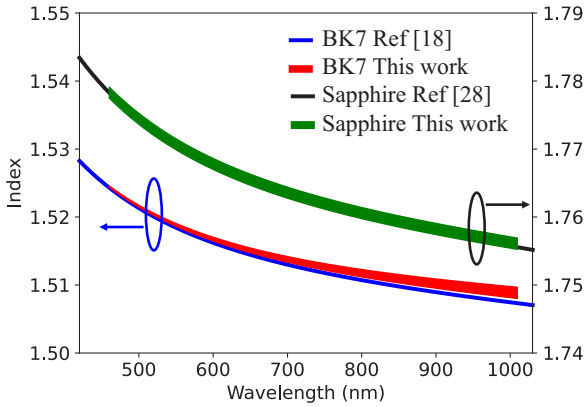

Fig. 7. Reconstructed indices of refraction for BK7 and sapphire n_o. The BK7 curves correspond to the left axis, while the sapphire corresponds to the right. The thickness in the lines are the uncertainty in the measurement.

index is lower. We find that the index for 1-decanol follows a similar curve to ethanol, but is approximately 0.03 higher across the spectrum.

We carried out this work at an ambient air temperature of 24°C with 40% humidity, in a temperature (< ± 1°C and humidity (<±5%)-controlled facility. The values for the constants in Eq. (4) are tabulated in Table 3. We note that for ethanol, the retrieved value for E is $<10^{-19}$ and did not affect the value for n. The measured indices of refraction for ethanol and 1-decanol are in good agreement with Ref. [29] at 25°C (red circle). Although the reported index temperature depedence in alcohols is 10^{-4}/°C at 589 nm, the discrepancy in the near infrared may be caused by a larger temperature dependence in this region. Our measurement for the index of refraction of 1-decanol is also in good agreement with Ref. [29] at 25°C (green circle).

By comparing the white light spectra of the two arms of the interferometer, we measure the transmission of 1-decanol in the 1 cm cuvette. In the transmission measurement, we divide the spectrum of the sample arm by the reference arm without a cuvette. The front and back reflections of the cuvette lead to an additional loss of $R \approx 3.5\%$ per surface, which we account for in the absorbance measurement. The absorbance is then calculated by $A = -log_{10}T/(1-R)^2$.

Optics EXPRESS

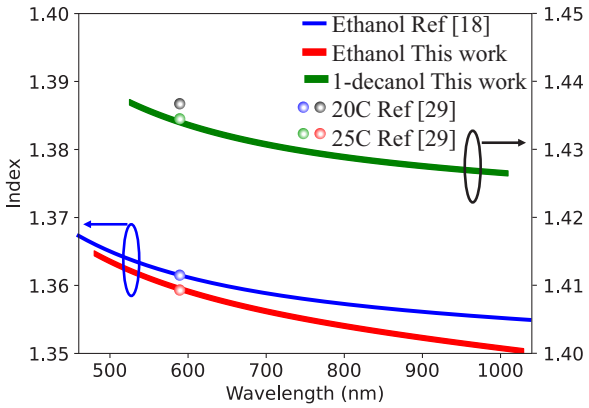

Fig. 8. Reconstructed indices of refraction for ethanol and 1-decanol. The ethanol curves correspond to the left axis, while the 1-decanol corresponds to the right. This work was carried out at 24°C.

Table 3. Coefficients for the indices of refraction for the measured samples.

Sample	A	B (10^3 nm^2)	C (10^{-9} nm^{-2})	D (10^7 nm^4)	E (10^{-16} nm^{-4})	F (10^{12} nm^6)
BK7	1.5066	3.7639	−1.8098	1.0433	−4.3697	1.7841
Sapphire n_o	1.7553	4.9392	−3.5055	1.5773	−4.0709	1.0438
Ethanol	1.3511	3.5070	−3.8207	−6.7926	0	6.2221
1-Decanol	1.4230	3.7347	−2.6465	1.9558	−2.5286	1.1905

The transmission and absorbance of 1-decanol are shown in Fig. 9. Although the absorbance is near zero for most of the visible portion of the spectrum, there is an absorption near 925 nm.

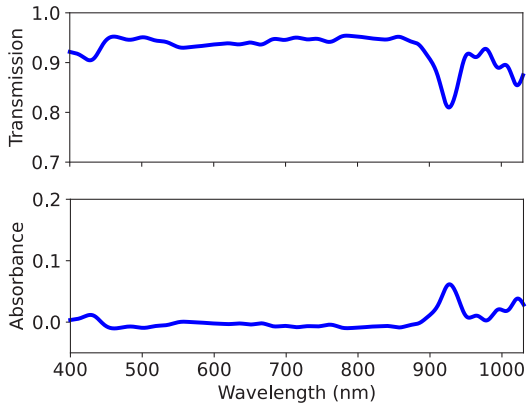

Fig. 9. Transmission and absorbance of 1-decanol in the visible and near infrared.

4. Conclusion

We measure the dispersion and the index of refraction of BK7, n_o sapphire, ethanol, and 1-decanol over the visible and near infrared regions using SRWLI. We find good agreement between our measurements and literature, and report for the first time to our knowledge the dispersion and index of refraction of 1-decanol. Once correcting for the stage positioning, the largest source of

Optics EXPRESS

error is the thickness of the samples, which leads to a relative error in the dispersion calculation of 0.1%. The weak absorption throughout the visible up to 900 nm makes 1-decanol a suitable candidate for supercontinuum generation from ultrafast visible and near infrared lasers.

Funding. Natural Sciences and Engineering Research Council of Canada (RGPIN-2019-06877); University of Windsor Xcellerate grant (5218522).

Acknowledgments. This project is in memory of Jill Crossman. We would like to thank Aldo DiCarlo for his technical assistance.

Disclosures. The authors declare no conflicts of interest.

Data availability. Data underlying the results presented in this paper are not publicly available at this time but may be obtained from the authors upon reasonable request.

References

1. J.-C. Diels, *Ultrashort Laser Pulse Phenomena* (Academic Press, 2006).
2. A. Wirth, M. T. Hassan, I. Grguraš, J. Gagnon, A. Moulet, T. T. Luu, S. Pabst, R. Santra, Z. A. Alahmed, A. M. Azzeer, V. S. Yakovlev, V. Pervak, F. Krausz, and E. Goulielmakis, "Synthesized light transients," Science **334**(6053), 195–200 (2011).
3. T. J. Hammond, D. Villeneuve, and P. B. Corkum, "Producing and controlling half-cycle near-infrared electric-field transients," Optica **4**(7), 826–830 (2017).
4. M. Lorenc, M. Zioloek, R. Naskrecki, J. Karolczak, J. Kubicki, and A. Maciejewski, "Artifacts in femtosecond transient absorption spectroscopy," Appl. Phys. B **74**(1), 19–27 (2002).
5. A. Stolow, A. E. Bragg, and D. M. Neumark, "Femtosecond time-resolved photoelectron spectroscopy," Chem. Rev. **104**(4), 1719–1758 (2004).
6. M. Na, A. K. Mills, F. Boschini, M. Michiardi, B. Nosarzewski, R. P. Day, E. Razzoli, A. Sheyerman, M. Schneider, G. Levy, S. Zhdanovich, T. P. Devereaux, A. F. Kemper, D. J. Jones, and A. Damascelli, "Direct determination of mode-projected electron-phonon coupling in the time domain," Science **366**(6470), 1231–1236 (2019).
7. T. J. Hammond, A. K. Mills, and D. J. Jones, "Simple method to determine dispersion of high-finesse optical cavities," Opt. Express **17**(11), 8998–9005 (2009).
8. F. Krausz and M. Ivanov, "Attosecond physics," Rev. Mod. Phys. **81**(1), 163–234 (2009).
9. R. A. Ganeev, C. Hutchison, A. Zaïr, T. Witting, F. Frank, W. A. Okell, J. W. G. Tisch, and J. P. Marangos, "Enhancement of high harmonics from plasmas using two-color pump and chirp variation of 1 khz ti:sapphire laser pulses," Opt. Express **20**(1), 90–100 (2012).
10. M. E. Corrales, J. González-Vázquez, G. Balerdi, I. R. Solá, R. de Nalda, and L. B. nares, "Control of ultrafast molecular photodissociation by laser-field-induced potentials," Nat. Chem. **6**(9), 785–790 (2014).
11. E. Neyra, F. Videla, J. A. Pérez-Hernánde, M. F. Ciappina, L. Roso, and G. A. Torchia, "High-order harmonic generation driven by chirped laser pulses induced by linear and non linear phenomena," Eur. Phys. J. D **70**(11), 243 (2016).
12. M. T. Hassan, T. T. Luu, A. Moulet, O. Raskazovskaya, P. Zhokhov, M. Garg, N. Karpowicz, A. M. Zheltikov, V. Pervak, F. Krausz, and E. Goulielmakis, "Optical attosecond pulses and tracking the nonlinear response of bound electrons," Nature **530**(7588), 66–70 (2016).
13. A. L. Guerrero, C. Sainz, H. Perrin, R. Castell, and J. Calatroni, "Refractive index distribution measurements by means of spectrally-resolved white-light interferometry," Opt. Laser Technol. **24**(6), 333–339 (1992).
14. C. Sainz, J. E. Calatroni, and G. Tribillon, "Refractometry of liquid samples with spectrally resolved white light interferometry," Meas. Sci. Technol. **1**(4), 356–361 (1990).
15. H. Delbarre, C. Przygodzki, M. Tassou, and D. Boucher, "High-precision indexmeasurement in anisotropic crystals using white-light spectral interferometry," Appl. Phys. B **70**(1), 45–51 (2000).
16. A. C. P. Rocha, J. R. Silva, S. M. Lima, L. A. O. Nunes, and L. H. C. Andrade, "Measurements of refractive indices and thermo-optical coefficients using a white-light michelson interferometer," Appl. Opt. **55**(24), 6639–6643 (2016).
17. Y. Arosa, E. López-Lago, L. M. Varela, and R. de la Fuente, "Spectrally resolved white light interferometry to measure material dispersion over a wide spectral band in a single acquisition," Opt. Express **24**(15), 17303–17312 (2016).
18. Y. Arosa, E. López-Lago, and R. de la Fuente, "Spectrally resolved white light interferometer for measuring dispersion in the visible and near infrared range," Measurement **122**, 6–13 (2018).
19. M. Galli, F. Marabelli, and G. Guizzetti, "Direct measurement of refractive-index dispersion of transparent media by white-light interferometry," Appl. Opt. **42**(19), 3910–3914 (2003).
20. S. H. Kim, S. H. Lee, J. I. Lim, and K. H. Kim, "Absolute refractive index measurement method over a broad wavelength region based on white-light interferometry," Appl. Opt. **49**(5), 910–914 (2010).
21. S. Diddams and J.-C. Diels, "Dispersion measurements with white-light interferometry," J. Opt. Soc. Am. B **13**(6), 1120–1129 (1996).
22. A. G. V. Engen, S. A. Diddams, and T. S. Clement, "Dispersion measurements of water with white-light interferometry," Appl. Opt. **37**(24), 5679–5686 (1998).

Optics EXPRESS

23. J. A. Stephen, C. J. Arachchige, and T. J. Hammond, "Spectral broadening for pulse compression using liquid alcohols," J. Phys. B: At., Mol. Opt. Phys. **55**(15), 155402 (2022).
24. N. Kanikkannan and M. Singh, "Skin permeation enhancement effect and skin irritation of saturated fatty alcohols," Int. J. Pharm. **248**(1-2), 219–228 (2002).
25. D. Ghosh, S. Batuta, N. A. Begumb, and D. Mandal, "Unusually slow intramolecular proton transfer dynamics of 4′-n, n-dimethylamino-3-hydroxyflavone in high n-alcohols: involvement of solvent relaxation," Photochem. Photobiol. Sci. **15**(2), 266–277 (2016).
26. C. Sainz, P. Jourdain, R. Escalona, and J. Calatroni, "Real time interferometric measurements of dispersion curves," Opt. Commun. **110**(3-4), 381–390 (1994).
27. D. X. Hammer, A. J. Welch, G. D. Noojin, R. J. Thomas, D. J. Stolarski, and B. A. Rockwell, "Spectrally resolved white-light interferometry for measurement of ocular dispersion," J. Opt. Soc. Am. A **16**(9), 2092 (1999).
28. I. H. Malitson, "Refraction and dispersion of synthetic sapphire," J. Opt. Soc. Am. **52**(12), 1377–1379 (1962).
29. J. Ortega, "Densities and refractive indices of pure alcohols as a function of temperature," J. Chem. Eng. Data **27**(3), 312–317 (1982).